



Preparation of hierarchically biomass from waste for regeneration of extracted organic phases

Bo Li^{1,3} · Jianing Zhu² · Shuya Wang² · Lulu Li² · Xinyuan Fang² · Siyu Gao² · Hong Zheng² · Wenping Cao² · Hongming Xu² · Youxian Zhang¹

Received: 27 March 2024 / Revised: 23 June 2024 / Accepted: 29 June 2024

© The Author(s), under exclusive licence to Springer-Verlag GmbH Germany, part of Springer Nature 2024

Abstract

The discharge of discarded organic phases often carries the risk of polluting the environment. The recycling and utilization of organic phases can reduce the negative impact on the environment and the consumption of natural resources. This manuscript reports a method for preparing biomass porous carbon using discarded mungbean pods and applying it to capacitive deionization (CDI) technology for organic phase regeneration. During the preparation process, porous carbon was prepared using potassium carbonate as an activator, NaCl/KCl mixed salt as a template and flux, and dopamine as a nitrogen source. The biomass-graded porous carbon prepared has a high specific surface area ($2862.36 \text{ m}^2 \text{ g}^{-1}$), rich pore structure, and good electrochemical performance (specific capacitance of 480.5 F g^{-1} at a current density of 1 A g^{-1}), making it suitable for ion adsorption and desorption processes in CDI technology. The CDI regeneration extraction organic phase experiment verified that the extraction ability of the regenerated extracted organic phase of the material in the extraction experiment can reach 99.6% of that of the fresh extractant. The results indicate that biomass-graded porous carbon has high ion adsorption capacity and good regeneration performance, which can achieve the recycling of organic phase.

Keywords Biomass-graded porous carbon · Capacitive deionization technology · Organic phase regeneration · Resource utilization

1 Introduction

The remaining organic phase after extraction usually contains substances that are harmful to human health and the environment. If such organic phases are directly discharged without treatment, it may cause serious harm to human

health and the ecological environment [1, 2]. Therefore, recycling the remaining organic phase after extraction is a sustainable approach that is of great significance for achieving dual economic and environmental benefits.

One of the methods for organic phase recycling is to wash and remove metal ions from the organic phase. The washing process requires multiple cycles and consumes a significant amount of water. Capacitive deionization technology is a method used to remove ions from water. Its principle is to use the double layer structure formed on the charged surface of the electrode to adsorb ions, while the charge carried by the ions is stored in the form of capacitance. The separation and removal of positive and negative ions can be achieved through the action of an electric field. The use of capacitive deionization technology for the recycling of organic phases may achieve good ion removal efficiency and reduce water consumption.

One of the key factors in capacitive deionization technology is the electrode material. Different types of electrode materials (transition metal alloy materials [3, 4], oxides [5–9], hydroxides [10, 11], and sulfides [12, 13], etc.) used

✉ Shuya Wang
wsy0414@163.com

✉ Youxian Zhang
zhangyx@lzu.edu.cn

¹ Key Laboratory of Western China's Environmental Systems (Ministry of Education) and Key Laboratory for Environmental Pollution Prediction and Control, College of Earth and Environmental Sciences, Lanzhou University, Lanzhou 730000, Gansu Province, China

² College of Environmental Engineering, Xuzhou University of Technology, Xuzhou 221018, China

³ Key Laboratory of Green and High-End Utilization of Salt Lake Resources, Qinghai Institute of Salt Lakes, Chinese Academy of Sciences, Xining 810008, China

for supercapacitors can be used in capacitive deionization technology. Carbon materials have attracted attention due to their high stability, easy preparation, low cost and conductivity [14]. Among them, biomass carbon materials are widely used to prepare electrodes because of their renewable, low cost and easy access [15, 16]. Biomass materials contain rich surface functional groups such as carbon, nitrogen, phosphorus and sulfur, and their structure is easily controlled during the reaction process [17, 18]. In addition, biomass materials have natural transport channels for water and nutrients, that is, they have natural porous structures suitable for charge storage [19–21]. As a result, as a carbon precursor for preparing electrode materials, biomass materials have attracted widespread attention in the industry.

The excellent adsorption performance of capacitive deionization technology cannot be achieved without the design of electrode materials. At present, the effective methods to obtain ideal carbon electrode materials include the pore structure design and element doping modification of the electrode materials [22, 23]. In terms of pore structure design, the best combination of macropores, mesopores, and micropores, that is, the construction of hierarchically porous carbon, is considered to be one of the promising and effective strategies to significantly improve the surface adsorption performance of carbon electrode materials [24]. Different types of pore structures will play their respective roles and improve the comprehensive performance of supercapacitors through the combination of different structures. Microholes provide effective storage of ions at the electrode/electrolyte energy storage interface [25]. The mesoporous channel facilitates the electrolyte diffusion and provides a channel for the ion diffusion in the electrolyte to enter the energy storage interface of the bulk material [26]. Macropores are used as electrolyte reservoir for shortening the distance of ion diffusion [27].

In addition to the construction of layered porous nanostructures with micropores, mesopores, and macropores mentioned above, another effective method to improve energy storage performance is the doping of heteroatoms in carbon materials improving the surface wettability of carbon materials and increasing the active energy storage sites [28–31]. Nitrogen atom doping has unique advantages in improving energy storage performance [32]. Nitrogen doping in the energy storage of porous carbon materials is mainly reflected in the following aspects. It is generally accepted that N doping can generate more active sites in the carbon skeleton [33, 34]. Additionally, N doping can optimize the contactable surface of the porous carbon electrode, so as to improve the surface wettability of the of aqueous electrolyte on porous carbon electrode surface [35–37].

In this manuscript, mungbean pods are selected as the precursor of carbon electrode materials because of their easy availability and large quantity. The porous carbon electrode

with graded porous structure was prepared by using the environmentally friendly K_2CO_3 pore-forming agent and the mixed flux of KCl/NaCl. In the preparation process, the addition of KCl/NaCl mixed flux can increase the contact area between K_2CO_3 pore forming agent and biomass material during the calcination process, thereby improving the pore forming efficiency. In addition, the addition of mixed fluxes can also provide a template effect in the formation process of porous carbon materials, which is conducive to the formation of porous structures. Dopamine, which is non-toxic and easily degradable, is used as a nitrogen source to achieve heterogeneous doping of porous carbon. The electrochemical performance of supercapacitors assembled from biomass-based carbon materials was studied in a three-electrode system. The excellent performance based on mungbean pods demonstrates the potential of this porous carbon material as a capacitive deionized electrode. And the processing ability was verified through experiments of regenerating and extracting organic phases.

2 Experimental section

2.1 Materials

Mungbean pods was collected from Weifang, Shandong Province, China, and used directly after washing with water several times. KCl, NaCl, and dopamine were purchased from Sinopharm Chemical Reagents Co., Ltd. All other chemical reagents are from Aladdin Reagent Co., Ltd.

2.2 Synthesis of porous carbon

Weigh the crushed biomass material, pore forming agent K_2CO_3 , flux NaCl, and flux KCl in a mass ratio of 1:3:3:3, and add nitrogen-containing dopamine (in a mass ratio of 1:100 to the biomass material) for solid-state grinding. Then, press the mixture into a cylindrical shape using a tablet press. Put the sample into a vacuum tube furnace and heat it to 850 °C under a nitrogen atmosphere according to the procedure, and keep it warm for 2 h. After calcination, wash the mixture to obtain N-doped porous carbon material, named PC-N. As a comparison, the porous carbon material prepared without adding a nitrogen source is named PC-0.

2.3 Structure and morphology characterization

Nitrogen adsorption–desorption isotherms were measured on a 4-station fully automatic specific surface area analyzer of the American Micromeritics APSP 2460 model under liquid nitrogen conditions at a temperature of 77 K. The specific surface area was also supplemented testing by mercury intrusion (Micromeritics Autopore V 9620). The morphological

characteristics of the Biomass porous carbon were mainly outlined by scanning electron microscopy (SEM, Hitachi Regulus 8100) and transmission electron microscope (TEM, Thermo Fisher Talos F200X). Thermo Scientific K-Alpha X-ray photoelectron spectroscopy (XPS) using Al K α rays as the excitation source to further aid in the specification of the structural information of the sample. Raman spectroscopy was performed using the Horiba LabRAM HR Evolution Raman spectrometer from Japan to analyze the structure of CDI electrode active materials.

2.4 Electrochemical characterization

In this manuscript, a three-electrode supercapacitor system was used to test the electrochemical performance of the carbon materials such as galvanostatic charge/discharge (GCD), cyclic voltammetry (CV), and electrochemical impedance spectroscopy (EIS). Hg/HgO and platinum sheets were used as reference electrode and counter electrode respectively, foam nickel coated with carbon materials was used as working electrode. Cyclic voltammetry, constant current charge–discharge and AC impedance tests were conducted at the electrochemical workstation of Shanghai Chenhua (CHI760E), and the frequency range of AC impedance test was 0.01–100000 Hz.

2.5 Treatment and analysis of organic extraction phase by CDI

The organic phase that needs to be regenerated in this article takes the extractant t-BAMPB after extracting rubidium as an example, and the process is shown in Fig. 1. Add the used organic extraction phase to the aqueous phase in a 2:1 volume ratio into a storage bottle, stir for a certain period of time, and let it stand to complete the layering. The aqueous phase in the storage bottle is introduced into the CDI device through a peristaltic pump, and an applied voltage is applied to form the electrostatic adsorption of ions in the water by

CDI. The adsorption results of ions are recorded through conductivity testing.

3 Results and discussion

3.1 Structural and morphological characterization

Figure 2 shows the process of preparing biomass porous carbon using mungbean pods as raw materials. The reagents added during the preparation process mainly include pore forming agent K₂CO₃, flux (KCl + NaCl), and dopamine, which provides a nitrogen source. The presence of flux can provide more possibilities for the full contact of pore forming agents and dopamine with raw materials during high-temperature calcination. In the subsequent calcination process, the flux will become molten near 700°C, creating favorable conditions for the occurrence of pore forming reactions. The introduction of nitrogen species can also generate functional groups on the surface of carbon materials, thereby enhancing their electronic conductivity, surface wettability, and pseudocapacitive interactions between proton and electron donor nitrogen atoms [38–40].

Figure 3 is a scanning electron microscope image of the prepared porous carbon material. Among them, Fig. 3a–c shows the morphology of porous materials PC-N prepared using dopamine nitrogen sources. Figure 3d–f shows a comparative morphology of PC-0 without the addition of a nitrogen source. Porous materials with certain pores can be prepared under both conditions. This can be attributed to the inherent nitrogen in mung bean pods, which can increase the surface adsorption between biomass and pore forming agents, thereby obtaining a porous morphology during the calcination process. Compared with materials without nitrogen sources, PC-N exhibits greater uniformity and integrity in their pore structure. This conclusion can be further validated on TEM comparative images (Fig. S1). The mapping diagram of PC-N material is shown in Fig. 3g–j, from which

Fig. 1 Schematic diagram of CDI device for regenerating organic phase

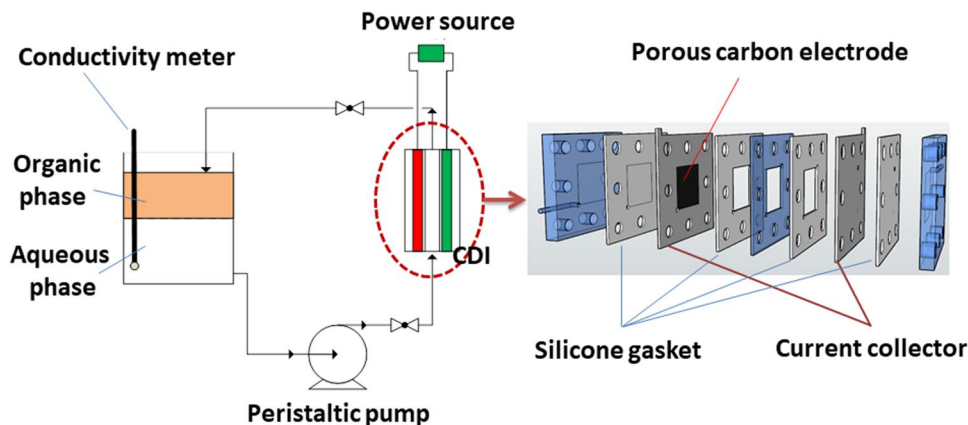


Fig. 2 Schematic diagram of preparation process of porous carbon

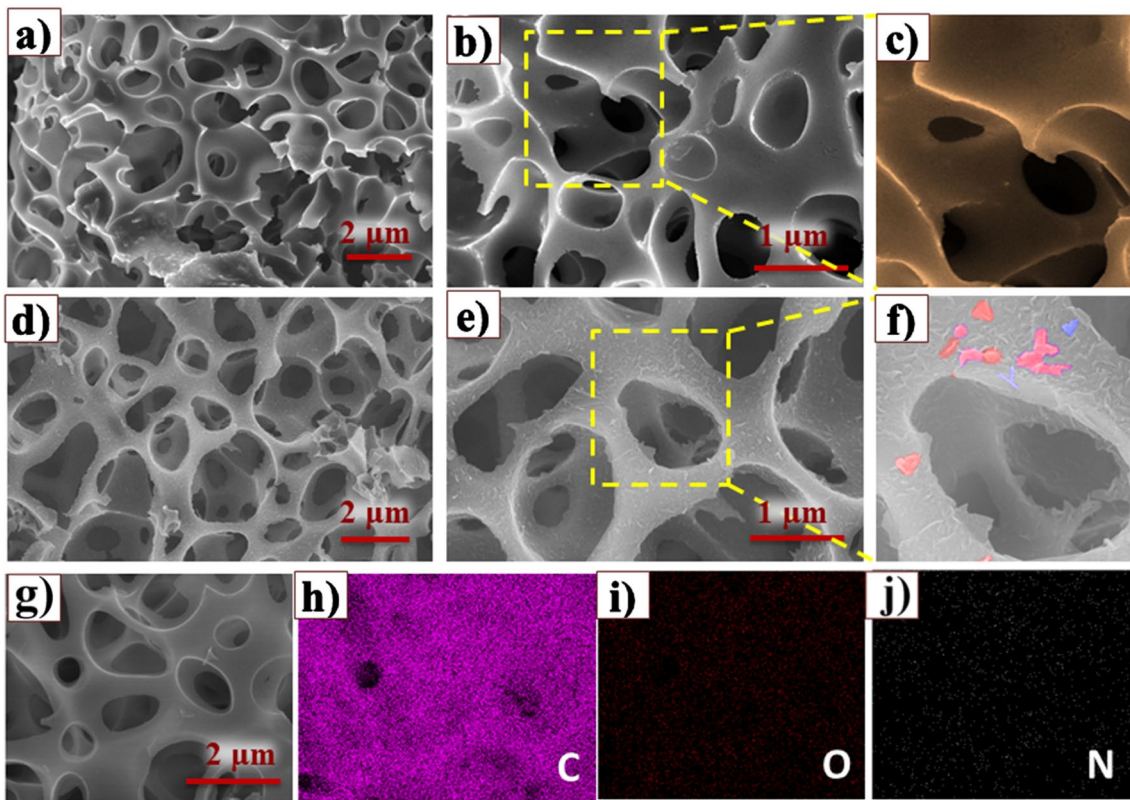
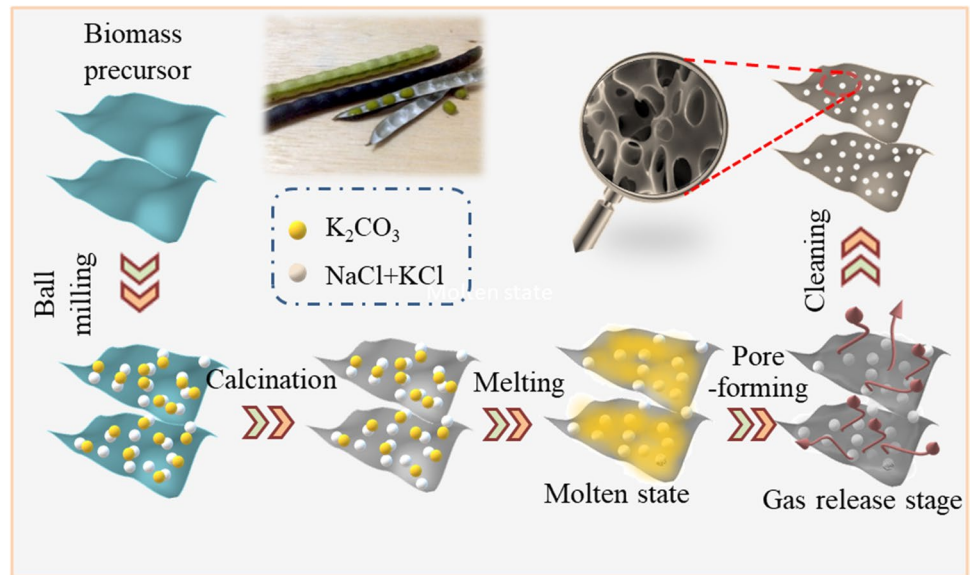


Fig. 3 SEM images of porous carbons(a-c: PC-N, d-f: PC-0, g-j: mapping of PC-N)

the presence and uniform distribution of C, N, and O elements can be clearly seen.

The differences in the morphology of the prepared materials can be explained by XPS (Fig. 4a–d). The high-resolution C1s, O1s, and N1s spectra of porous carbon PC-N indicate that the prepared porous carbon contains abundant

functional groups of C, O, and N elements. The presence of these functional groups not only benefits the surface wettability and hydrophilicity of the porous carbon, but also indicates that the electrode has the ability to coordinate with ions, thereby promoting electro adsorption [41]. There are three distinct peaks in the N 1s spectrum, corresponding to

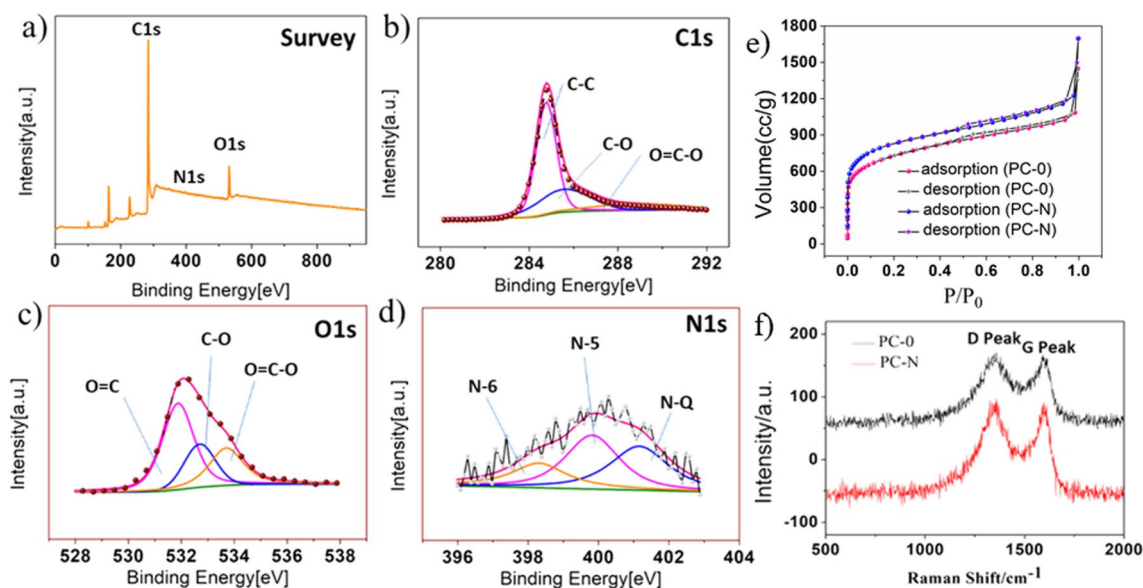


Fig. 4 Structural characterization of biomass porous carbon (a: XPS Survey of PC-N. b–d: high-resolution spectra of C1s, O1s, and N1s of PC-N. e: Adsorption and desorption curves of BET test of PC-0 and PC-N. f: Raman spectrogram of PC-0 and PC-N)

pyrrole nitrogen (N-6), pyridine nitrogen (N-5), and quaternary nitrogen (N-Q). The presence of pyridine N can enhance the Lewis alkalinity and can increase the proportion of sp^2 hybrid structures of the material surface, thereby increasing the wettability of the material surface and contributing to the generation of pseudocapacitance [42–44]. Compared with PC-0 (Fig. S2), PC-N has a higher content of pyridine-N, which generates more active sites to store charges, significantly improving the pseudocapacitive properties of carbon materials.

In theory, there is a close relationship between the specific surface area and specific capacity of electrode materials. However, a more accurate statement of this viewpoint is to accurately represent the specific surface area as the “effective specific surface area” of the electrode material [45, 46]. When the ion diameter of the electrolyte is fully compatible with the pore structure, the highest capacity can be achieved [47]. According to density functional theory simulations, as the temperature decreases, ions are difficult to desolvate, so pore structures larger than solvated ions can better participate in energy storage [48]. In addition, in order to realize efficient energy storage of porous materials, researchers also realized that mesopores as ion transport channels are indispensable. Its existence can not only store large solvated ions, but also shorten the ion transport path, reduce the ion transport impedance, and greatly optimize the multiplier performance and cycle performance of the device [49, 50]. Combining the above two points of view, the construction of micro/mesoporous hierarchical porous structure suitable for electrolyte ions becomes one of the key factors to optimize electrode materials. The isotherm

of biomass porous carbon can be observed (Fig. 4e), and when the relative pressure is low, the adsorption curve of the sample rapidly increases, indicating the presence of abundant micropores in the material. The hysteresis loop generated in the curve with increasing pressure confirms the existence of mesopores. The presence of micropores and mesopores can achieve full electrochemical performance. Compared with PC-0 ($2512.22 \text{ m}^2 \text{ g}^{-1}$), PC-N has a higher specific surface area ($2862.36 \text{ m}^2 \text{ g}^{-1}$), which is beneficial for its electrochemical performance. The distribution of pore structure and structural parameters are shown in Fig. S3 and Tab. S1. Additionally, the crystalline structure of the PC-0 and PC-N were studied by Raman spectroscopy (Fig. 4f). Obviously, Raman spectroscopy shows that both samples have two characteristic bands, the G peak and the D peak. The PC-N showed a higher intensity ratio ($I_D/I_G=0.93$) than that of PC-0 ($I_D/I_G=0.90$), indicating that more defects were induced by nitrogen doping.

3.2 Electrochemical performance characterization

Figure 5 shows the GCD and CV curves of the porous carbon electrode in a three-electrode system. The GCD curves of PC-N and PC-0 at a current density of 2 A g^{-1} in the voltage range of 1 V to 0 V are shown in Fig. 5a. The specific capacitance of PC-0 and PC-N at a current density of 2 A g^{-1} is 380.0 and 451.8 F g^{-1} , respectively. The GCD data of two electrodes at different current densities are shown in Fig. 5b and 5c, respectively. The GCD curve of PC-0 electrode (Fig. 5b) is a symmetrical triangle, thus confirming the typical double layer capacitance behavior. For the same

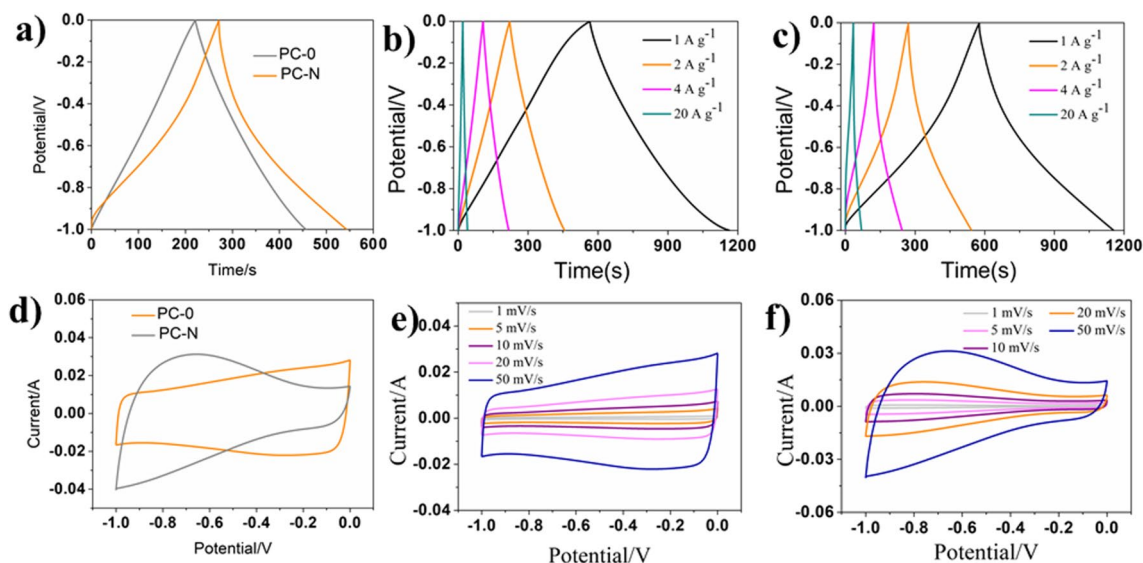


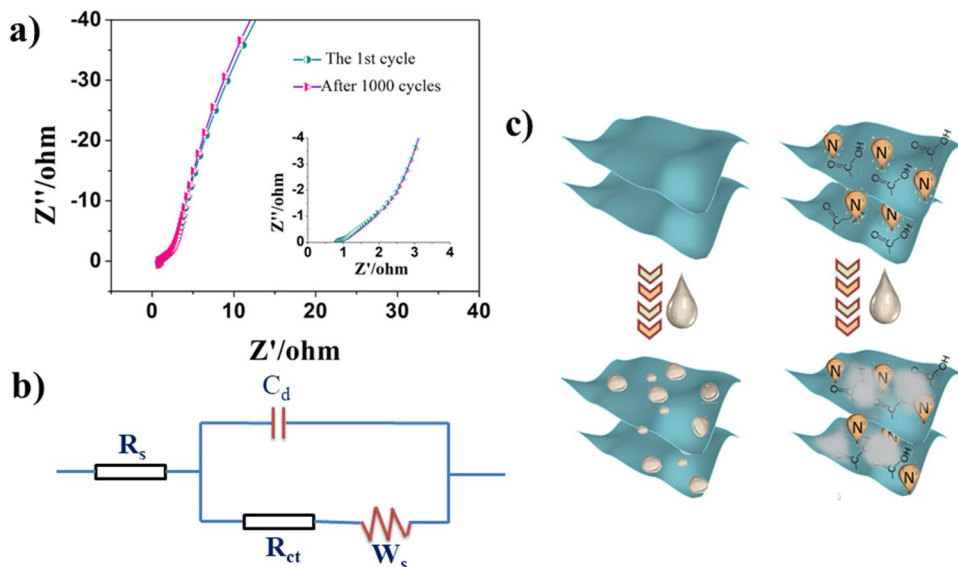
Fig. 5 GCD profiles (a: GCD curves of PC-N and PC-0 at 2 A g^{-1} , b: PC-0, c: PC-N) at different current densities and CV curves (d: CV curves at 50 mV/s , e: PC-0, f: PC-N) at different scan rates

specific current, PC-N electrode materials exhibit higher specific capacitance values and certain pseudocapacitive behavior. For PC-N electrodes (Fig. 5c), the specific electrical capacities at 1 A g^{-1} , 2 A g^{-1} , 4 A g^{-1} , and 20 A g^{-1} are 480.5 F g^{-1} , 451.8 F g^{-1} , 406.3 F g^{-1} , and 359.8 F g^{-1} , respectively. As the current density increases, the diffusion resistance of charges in the pore structure increases, leading to a decrease in specific capacity. Figure 5d shows the comparison of CV curves between PC-0 and PC-N electrodes in the voltage range of -1 V to 0 V at a scanning speed of 50 mV/s . Figure 5e and 5f show CV images of PC-0 and PC-N electrodes collected at different scanning rates, respectively. The rectangular CV curve also confirms

the ideal EDLC behavior of the PC-0 electrode. The pseudocapacitive behavior of PC-N electrode mainly comes from the nitrogen doping behavior of PC-N electrodes, which can accelerate the ion transmission speed, provide more active sites and improve the wettability of the interface [51].

EIS was used to further study the interface characteristics of the porous carbon electrodes [52]. Figure 6a shows a comparison of the Nyquist plot of the PC-N electrode after the first cycle and 1000 cycles. After 1000 charge discharge cycles, the stability of the electrochemical impedance spectrum is high, which also confirms the cycling stability of the material. The corresponding circuit diagram is shown in Fig. 6b. The low-frequency region of the Nyquist diagram

Fig. 6 Nyquist plots of porous carbon electrodes. (a: Comparison of Nyquist diagram PC-N electrodes after the first and 1000 cycles; b: Equivalent-circuit diagram; c: The mechanism of improving stability)



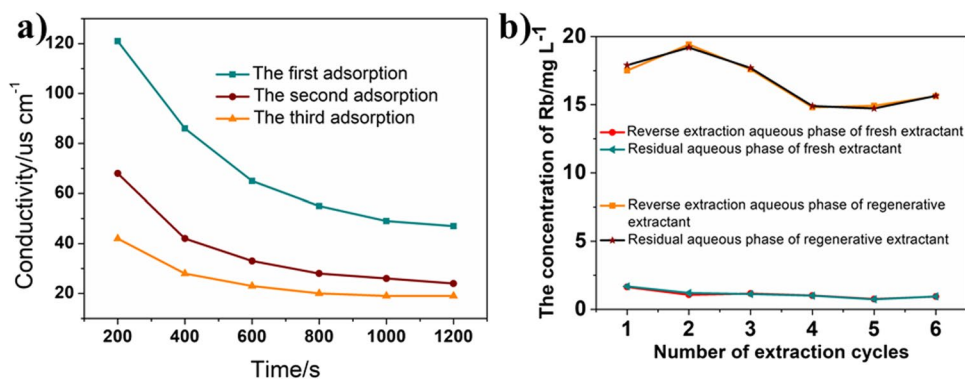
indicates the pseudocapacitive behaviour of the carbon electrode. The semicircle in the low frequency region also confirmed the more obvious pseudo-capacitance behavior. The cyclic stability of PC-N comes from functional groups such as carboxyl groups on the surface of the material itself, as well as nitrogen doping during the preparation process, which increases the wettability of the material surface (Fig. 6c).

3.3 Analysis of regeneration treatment results for organic phase extraction

The organic phase that needs to be regenerated will undergo three water washing and electro adsorption experiments. When the charging voltage is 1.2 V, the trend of the conductivity of the porous carbon electrode over time is shown in Fig. 7a. After applying the charging voltage, the conductivity of the solution decreases rapidly at a low speed, indicating that the ions in the solution are adsorbed onto the electrode with opposite charges by the electric field. Subsequently, the conductivity of the solution slowly decreased and stabilized within 20 min, reaching the electro adsorption equilibrium. The desorption process of ions is achieved under reverse voltage or short circuit conditions. After three adsorption cycles, the conductivity of the solution can be reduced to $19 \mu\text{S cm}^{-1}$.

In order to investigate whether the extractant t-BAMBP can be recycled, the extraction conditions were chosen to be the same as those of fresh extractants. Based on the comparison of ion concentrations in the residual aqueous phase and the reverse extraction aqueous phase, the conclusion can be drawn as to whether the extractant can be regenerated. From the Fig. 7b, it can be seen that the extraction ability of t-BAMBP recycled has not decreased. After 6 extraction-counter extraction cycles, the extraction capacity of the recovered extractant can reach 99.6% of that of fresh extractants. This indicates that the extractant can be recycled, which has significant theoretical value and economic significance for industrial application.

Fig. 7 Relevant data on the regeneration of organic phases using capacitive deionization technology. (a: The variation of conductivity under different cycle times. b: Comparison of extraction data between regenerated organic phase and fresh organic phase)



4 Conductions

This manuscript successfully prepared biomass-graded porous carbon using discarded pods and applied it to the organic phase regeneration technology of CDI technology. This solves the problem of handling agricultural waste, and this process of turning waste into treasure is precisely the goal pursued by the current circular economy and sustainable development. This manuscript used potassium carbonate as an activator and NaCl/KCl as a mixed flux to prepare porous carbon, which had a high specific surface area, rich pore structure, and good electrochemical performance, suitable for ion adsorption and desorption processes in CDI technology. This study proposes a new solution for the application of CDI technology in organic phase regeneration. After 6 extraction-counter extraction cycles, the extraction capacity of the recovered extractant can reach 99.6% of that of fresh extractants. By comparing the usage data of regenerated organic phase and fresh organic phase, the actual effect of this method on regenerated organic matter was further verified. Therefore, this method has practical application value and is expected to provide an effective way for the treatment and resource utilization of waste organic phases. In addition, this method has the advantages of low cost and environmental friendliness, providing new ideas for the utilization of waste resources and the development of CDI technology.

Supplementary Information The online version contains supplementary material available at <https://doi.org/10.1007/s13399-024-05905-7>.

Author contribution Bo Li: Investigation, Data curation, Writing—original draft.

Jianing Zhu: Investigation, Methodology.

Shuya Wang: Writing—review & editing, Supervision, Methodology.

Lulu Li: Visualization, Data curation.

Xinyuan Fang: Data curation and Software.

Siyu Gao: Methodology and Validation.

Hong Zheng: Data curation and Validation.

Wenping Cao: Validation, Supervision.

Hongming Xu: Methodology and Validation.

Youxian Zhang: Writing—review & editing, Supervision.

Funding This work was kindly supported by the National Key R&D Program of China (No. 2023YFC2908200) and Natural Science Foundation of China (No. U22A20411).

Declarations

Conflict of interest The authors declare no competing interests.

References

- Lu D, Li P, Xiao W, He G, Jiang X (2017) Simultaneous recovery and crystallization control of saline organic wastewater by membrane distillation crystallization. *AIChE J* 63:2187–2197. <https://doi.org/10.1002/aic.15581>
- Abdulrahman A, van Walsum GP, Um B-H (2019) Acetic Acid Removal from Pre-Pulping Wood Extract with Recovery and Recycling of Extraction Solvents. *Appl Biochem Biotechnol* 187:378–395. <https://doi.org/10.1007/s12010-018-2826-z>
- Chen M-X, Zhu M, Zuo M, Chu S-Q, Zhang J, Wu Y, Liang H-W, Feng X (2020) Identification of Catalytic Sites for Oxygen Reduction in Metal/Nitrogen-Doped Carbons with Encapsulated Metal Nanoparticles. *Angew Chem Int Ed* 59:1627–1633. <https://doi.org/10.1002/anie.201912275>
- Kong K, Hyun J, Kim Y, Kim W, Kim D (2019) Nanoporous structure synthesized by selective phase dissolution of AlCo-CrFeNi high entropy alloy and its electrochemical properties as supercapacitor electrode. *J Power Sources* 437:226927. <https://doi.org/10.1016/j.jpowsour.2019.226927>
- Zhu X, Hou D, Tao H, Li M (2020) Simply synthesized N-doped carbon supporting Fe₃O₄ nanocomposite for high performance supercapacitor. *J Alloy Compd* 821:153580. <https://doi.org/10.1016/j.jallcom.2019.153580>
- MohdAbdah MAA, Azman NHN, Kulandaivalu S, Sulaiman Y (2020) Review of the use of transition-metal-oxide and conducting polymer-based fibres for high-performance supercapacitors. *Mater Des* 186:108199. <https://doi.org/10.1016/j.matdes.2019.108199>
- Wang T, Chen HC, Yu F, Zhao XS, Wang H (2019) Boosting the cycling stability of transition metal compounds-based supercapacitors. *Energy Storage Mater* 16:545–573. <https://doi.org/10.1016/j.ensm.2018.09.007>
- Lu K, Song B, Li K, Zhang J, Ma H (2017) Cobalt hexacyanoferrate nanoparticles and MoO₃ thin films grown on carbon fiber cloth for efficient flexible hybrid supercapacitor. *J Power Sources* 370:98–105. <https://doi.org/10.1016/j.jpowsour.2017.10.012>
- Wang G, Xu H, Lu L, Zhao H (2014) Magnetization-induced double-layer capacitance enhancement in active carbon/Fe₃O₄ nanocomposites. *J Energy Chem* 23:809–815. [https://doi.org/10.1016/S2095-4956\(14\)60216-3](https://doi.org/10.1016/S2095-4956(14)60216-3)
- Hu H, Liu J, Xu Z, Zhang L, Cheng B, Ho W (2019) Hierarchical porous Ni/Co-LDH hollow dodecahedron with excellent adsorption property for Congo red and Cr(VI) ions. *Appl Surf Sci* 478:981–990. <https://doi.org/10.1016/j.apsusc.2019.02.008>
- Yao P, Li Z, Zhu J, Ran X, Shi Z, Zhu J (2021) Controllable synthesis of NiCo-LDH/Co(OH)₂@PPY composite via electrodeposition at high deposition voltages for high-performance supercapacitors. *J Alloy Compd* 875:160042. <https://doi.org/10.1016/j.jallcom.2021.160042>
- Qin Y, Lyu Y, Chen M, Lu Y, Qi P, Wu H, Sheng Z, Gan X, Chen Z, Tang Y (2021) Nitrogen-doped Ni₂P/Ni₁₂P₅/Ni₃S₂ three-phase heterostructure arrays with ultrahigh areal capacitance for high-performance asymmetric supercapacitor. *Electrochim Acta* 393:139059. <https://doi.org/10.1016/j.electacta.2021.139059>
- Chen H, Jiang J, Zhao Y, Zhang L, Guo D, Xia D (2015) One-pot synthesis of porous nickel cobalt sulphides: tuning the composition for superior pseudocapacitance. *J Mater Chem A* 3:428–437. <https://doi.org/10.1039/C4TA04420G>
- Song Y, Wang H, Cheng X, Li G, Chen X, Chen H, Miao L, Zhang X, Zhang H (2019) High-efficiency self-charging smart bracelet for portable electronics. *Nano Energy* 55:29–36. <https://doi.org/10.1016/j.nanoen.2018.10.045>
- Jung S, Shetti NP, Reddy KR, Nadagouda MN, Park Y-K, Aminabhavi TM, Kwon EE (2021) Synthesis of different biofuels from livestock waste materials and their potential as sustainable feedstocks – A review. *Energy Convers Manage* 236:114038. <https://doi.org/10.1016/j.enconman.2021.114038>
- Yin Y, Liu Q, Wang J, Zhao Y (2022) Recent insights in synthesis and energy storage applications of porous carbon derived from biomass waste: A review. *Int J Hydrogen Energy* 47:39338–39363. <https://doi.org/10.1016/j.ijhydene.2022.09.121>
- Yin Y, Liu Q, Zhao Y, Chen T, Wang J, Gui L, Lu C (2023) Recent Progress and Future Directions of Biomass-Derived Hierarchical Porous Carbon: Designing. *Prep Supercapacitor Appl Energy Fuel* 37:3523–3554. <https://doi.org/10.1021/acs.energyfuels.2c04093>
- Srivastava RK, Shetti NP, Reddy KR, Nadagouda MN, Badawi M, Bonilla-Petriciolet A, Aminabhavi TM (2023) Valorization of biowastes for clean energy production, environmental depollution and soil fertility. *J Environ Manage* 332:117410. <https://doi.org/10.1016/j.jenvman.2023.117410>
- Yang S, Wang S, Liu X, Li L (2019) Biomass derived interconnected hierarchical micro-meso-macro- porous carbon with ultrahigh capacitance for supercapacitors. *Carbon* 147:540–549. <https://doi.org/10.1016/j.carbon.2019.03.023>
- Zhan Y, Bai J, Guo F, Dong K, Shu R, Liu S, Qiao Q, Xu L (2022) Manganese/copper bimetal-decorated biomass porous carbons as advanced electrode materials for high-performance supercapacitors. *J Energy Storage* 55:105636. <https://doi.org/10.1016/j.est.2022.105636>
- Khan A, Senthil RA, Pan J, Osman S, Sun Y, Shu X (2020) A new biomass derived rod-like porous carbon from tea-waste as inexpensive and sustainable energy material for advanced supercapacitor application. *Electrochim Acta* 335:135588. <https://doi.org/10.1016/j.electacta.2019.135588>
- Pilger F, Testino A, Carino A, Proff C, Kambolis A, Cervellino A, Ludwig C (2016) Size Control of Pt Clusters on CeO₂ Nanoparticles via an Incorporation-Segregation Mechanism and Study of Segregation Kinetics. *ACS Catal* 6:3688–3699. <https://doi.org/10.1021/acscatal.6b00934>
- Benzigar MR, Talapaneni SN, Joseph S, Ramadass K, Singh G, Scaranto J, Ravon U, Al-Bahily K, Vinu A (2018) Recent advances in functionalized micro and mesoporous carbon materials: synthesis and applications. *Chem Soc Rev* 47:2680–2721. <https://doi.org/10.1039/C7CS00787F>
- Ghosh A, Lee YH (2012) Carbon-Based Electrochemical Capacitors. *ChemSuschem* 5:480–499. <https://doi.org/10.1002/cssc.201100645>
- Shang Z, An X, Zhang H, Shen M, Baker F, Liu Y, Liu L, Yang J, Cao H, Xu Q, Liu H, Ni Y (2020) Houttuynia-derived nitrogen-doped hierarchically porous carbon for high-performance supercapacitor. *Carbon* 161:62–70. <https://doi.org/10.1016/j.carbon.2020.01.020>
- Taer E, Apriwandi A, Agustino A, Dewi MR, Taslim R (2022) Porous hollow biomass-based carbon nanofiber/nanosheet for high-performance supercapacitor. *Int J Energy Res* 46:1467–1480. <https://doi.org/10.1002/er.7262>
- Huang S, Ding Y, Li Y, Han X, Xing B, Wang S (2021) Nitrogen and Sulfur Co-doped Hierarchical Porous Biochar Derived from the Pyrolysis of Mantis Shrimp Shell for Supercapacitor

- Electrodes. *Energy Fuel* 35:1557–1566. <https://doi.org/10.1021/acs.energyfuels.0c04042>
28. Yue X, Yang H, An P, Gao Z, Li H, Ye F (2022) Multi-element co-doped biomass porous carbon with uniform cellular pores as a supercapacitor electrode material to realise high value-added utilisation of agricultural waste. *Dalton Trans* 51:12125–12136. <https://doi.org/10.1039/D2DT01750D>
 29. Lei X, Pan F, Hua C, Wang S, Xiong B, Liu Y, Fu Z, Xiang B, Lu Y (2022) Oxide-doped hierarchically porous carbon for high-performance supercapacitor. *J Alloy Compd* 901:163624. <https://doi.org/10.1016/j.jallcom.2022.163624>
 30. Yuan Z, Li J, Yang M, Fang Z, Jian J, Yu D, Chen X, Dai L (2019) Ultrathin Black Phosphorus-on-Nitrogen Doped Graphene for Efficient Overall Water Splitting: Dual Modulation Roles of Directional Interfacial Charge Transfer. *J Am Chem Soc* 141:4972–4979. <https://doi.org/10.1021/jacs.9b00154>
 31. Peng X, Zhang L, Chen Z, Zhong L, Zhao D, Chi X, Zhao X, Li L, Lu X, Leng K, Liu C, Liu W, Tang W, Loh KP (2019) Hierarchically Porous Carbon Plates Derived from Wood as Bifunctional ORR/OER Electrodes. *Adv Mater* 31:1900341. <https://doi.org/10.1002/adma.201900341>
 32. Mirzaei M, Abbas Q, Gibson D, Mazur M (2019) Effect of nitrogen doping on the electrochemical performance of resorcinol-formaldehyde based carbon aerogels as electrode material for supercapacitor applications. *Energy* 173:809–819. <https://doi.org/10.1016/j.energy.2019.02.108>
 33. Yang W, Zhou J, Wang S, Zhang W, Wang Z, Lv F, Wang K, Sun Q, Guo S (2019) Freestanding film made by necklace-like N-doped hollow carbon with hierarchical pores for high-performance potassium-ion storage. *Energy Environ Sci* 12:1605–1612. <https://doi.org/10.1039/C9EE00536F>
 34. Sun Z, Yang L, Zhang D, Song W (2019) High performance, flexible and renewable nano-biocomposite artificial muscle based on mesoporous cellulose/ ionic liquid electrolyte membrane. *Sens Actuators, B Chem* 283:579–589. <https://doi.org/10.1016/j.snb.2018.12.073>
 35. Xue D, Zhu D, Xiong W, Cao T, Wang Z, Lv Y, Li L, Liu M, Gan L (2019) Template-Free, Self-Doped Approach to Porous Carbon Spheres with High N/O Contents for High-Performance Supercapacitors. *ACS Sustain Chem Eng* 7:7024–7034. <https://doi.org/10.1021/acssuschemeng.8b06774>
 36. Ferrero GA, Fuertes AB, Sevilla M (2015) N-doped porous carbon capsules with tunable porosity for high-performance supercapacitors. *J Mater Chem A* 3:2914–2923. <https://doi.org/10.1039/C4TA06022A>
 37. Sun F, Gao J, Pi X, Wang L, Yang Y, Qu Z, Wu S (2017) High performance aqueous supercapacitor based on highly nitrogen-doped carbon nanospheres with unimodal mesoporosity. *J Power Sources* 337:189–196. <https://doi.org/10.1016/j.jpowsour.2016.10.086>
 38. Yin L-C, Liang J, Zhou G-M, Li F, Saito R, Cheng H-M (2016) Understanding the interactions between lithium polysulfides and N-doped graphene using density functional theory calculations. *Nano Energy* 25:203–210. <https://doi.org/10.1016/j.nanoen.2016.04.053>
 39. Ahmed N, Amer A, Ali BA, Biby AH, Mesbah YI, Allam NK (2020) Boosting the cyclic stability and supercapacitive performance of graphene hydrogels via excessive nitrogen doping: Experimental and DFT insights. *Sustain Mater Technol* 25:e00206. <https://doi.org/10.1016/j.susmat.2020.e00206>
 40. Wiener CG, Qiang Z, Xia Y, Tyagi M, Vogt BD (2018) Impact of surface wettability on dynamics of supercooled water confined in nitrogen-doped ordered mesoporous carbon. *Phys Chem Chem Phys* 20:28019–28025. <https://doi.org/10.1039/C8CP05670F>
 41. Xu D, Tong Y, Yan T, Shi L, Zhang D (2017) N, P-Codoped Meso-/Microporous Carbon Derived from Biomass Materials via a Dual-Activation Strategy as High-Performance Electrodes for Deionization Capacitors. *ACS Sustain Chem Eng* 5:5810–5819. <https://doi.org/10.1021/acssuschemeng.7b00551>
 42. Wang X, Pan H, Lin Q, Wu H, Jia S, Shi Y (2019) One-Step Synthesis of Nitrogen-Doped Hydrophilic Mesoporous Carbons from Chitosan-Based Triconstituent System for Drug Release. *Nanoscale Res Lett* 14:259. <https://doi.org/10.1186/s11671-019-3075-y>
 43. Yang P, Huang N, Leng YX, Yao ZQ, Zhou HF, Maitz M, Leng Y, Chu PK (2006) Wettability and biocompatibility of nitrogen-doped hydrogenated amorphous carbon films: Effect of nitrogen. *Nucl Instrum Methods Phys Res Sect B* 242:22–25. <https://doi.org/10.1016/j.nimb.2005.08.081>
 44. Zhu M, Chen Q, Kan J, Tang J, Wei W, Lin J, Li S (2019) Cobalt Oxide Nanoparticles Embedded in N-Doped Porous Carbon as an Efficient Electrode for Supercapacitor. *Energy Technol* 7:1800963. <https://doi.org/10.1002/ente.201800963>
 45. Wang Q, Yan J, Fan Z (2016) Carbon materials for high volumetric performance supercapacitors: Design, progress, challenges and opportunities. *Energy Environ Sci* 9:729–762. <https://doi.org/10.1039/C5EE03109E>
 46. Thommes M, Kaneko K, Neimark AV, Olivier JP, Rodriguez-Reinoso F, Rouquerol J, Sing KSW (2015) Physisorption of gases, with special reference to the evaluation of surface area and pore size distribution (IUPAC Technical Report). *Pure Appl Chem* 87:1051–1069. <https://doi.org/10.1515/pac-2014-1117>
 47. Raymundo-Piñero E, Kierzek K, Machnikowski J, Béguin F (2006) Relationship between the nanoporous texture of activated carbons and their capacitance properties in different electrolytes. *Carbon* 44:2498–2507. <https://doi.org/10.1016/j.carbon.2006.05.022>
 48. Xu J, Yuan N, Razal JM, Zheng Y, Zhou X, Ding J, Cho K, Ge S, Zhang R, Gogotsi Y, Baughman RH (2019) Temperature-independent capacitance of carbon-based supercapacitor from –100 to 60 °C. *Energy Storage Mater* 22:323–329. <https://doi.org/10.1016/j.ensm.2019.02.016>
 49. Song K, Li W, Xin J, Zheng Y, Chen X, Yang R, Lv W, Li Q (2021) Hierarchical porous heterostructured Co(OH)₂/CoSe₂ nanoarray: A controllable design electrode for advanced asymmetrical supercapacitors. *Chem Eng J* 419:129435. <https://doi.org/10.1016/j.cej.2021.129435>
 50. Yan R, Antonietti M, Oschatz M (2018) Toward the Experimental Understanding of the Energy Storage Mechanism and Ion Dynamics in Ionic Liquid Based Supercapacitors. *Adv Energy Mater* 8:1800026. <https://doi.org/10.1002/aenm.201800026>
 51. Zhou H, Shu R, Guo F, Bai J, Zhan Y, Chen Y, Qian L (2021) N-O-P co-doped porous carbon aerogel derived from low-cost biomass as electrode material for high-performance supercapacitors. *Diam Relat Mater* 120:108614. <https://doi.org/10.1016/j.diamond.2021.108614>
 52. Dong S, He X, Zhang H, Xie X, Yu M, Yu C, Xiao N, Qiu J (2018) Surface modification of biomass-derived hard carbon by grafting porous carbon nanosheets for high-performance supercapacitors. *J Mater Chem A* 6:15954–15960. <https://doi.org/10.1039/C8TA04080J>

Publisher's Note Springer Nature remains neutral with regard to jurisdictional claims in published maps and institutional affiliations.

Springer Nature or its licensor (e.g. a society or other partner) holds exclusive rights to this article under a publishing agreement with the author(s) or other rightsholder(s); author self-archiving of the accepted manuscript version of this article is solely governed by the terms of such publishing agreement and applicable law.